EXHIBIT
22

Large endolymphatic potentials from low-frequency and infrasonic tones in the guinea pig

Alec N. Salt,[a] Jeffery T. Lichtenhan, Ruth M. Gill, and Jared J. Hartsock
Department of Otolaryngology, Washington University School of Medicine, St. Louis, Missouri 63110

(Received 1 August 2012; revised 12 December 2012; accepted 9 January 2013)

Responses of the ear to low-frequency and infrasonic sounds have not been extensively studied. Understanding how the ear responds to low frequencies is increasingly important as environmental infrasounds are becoming more pervasive from sources such as wind turbines. This study shows endolymphatic potentials in the third cochlear turn from acoustic infrasound (5 Hz) are larger than from tones in the audible range (e.g., 50 and 500 Hz), in some cases with peak-to-peak amplitude greater than 20 mV. These large potentials were suppressed by higher-frequency tones and were rapidly abolished by perilymphatic injection of KCl at the cochlear apex, demonstrating their third-turn origins. Endolymphatic iso-potentials from 5 to 500 Hz were enhanced relative to perilymphatic potentials as frequency was lowered. Probe and infrasonic bias tones were used to study the origin of the enhanced potentials. Potentials were best explained as a saturating response summed with a sinusoidal voltage (V_o), that was phase delayed by an average of 60° relative to the biasing effects of the infrasound. V_o is thought to arise indirectly from hair cell activity, such as from strial potential changes caused by sustained current changes through the hair cells in each half cycle of the infrasound. © *2013 Acoustical Society of America*.
[http://dx.doi.org/10.1121/1.4789005]

PACS number(s): 43.64.Nf [CAS] Pages: 1561–1571

I. INTRODUCTION

The ear possesses numerous mechanisms to reduce the sensitivity to low-frequency sounds. Mechanically, the middle ear attenuates low-frequency sounds by ~6 dB/octave as frequency is lowered below 1 kHz (Dallos, 1973; Cheatham and Dallos, 2001). The helicotrema shunts pressure between scala tympani (ST) and scala vestibuli, attenuating low-frequency stimulation by ~6 dB/octave below 100 Hz both in humans (Dallos, 1970) and in guinea pigs (Franke and Dancer, 1982; Salt and Hullar, 2010). The stereocilia of the inner hair cells (IHCs) are not directly coupled to the tectorial membrane but are stimulated by fluid movements in the subtectorial space (Nowotny and Gummer, 2006; Guinan, 2012); this causes IHCs to be sensitive to basilar membrane velocity and attenuates low-frequency input by 6 dB/octave below ~470 Hz (Cheatham and Dallos, 2001). As hearing is mediated by IHCs, these mechanisms combine to make hearing very insensitive to low-frequency sounds and infrasound. As an example, a 5 Hz tone must be presented at ~109 dB SPL for humans to hear it (Møller and Pederson, 2004).

The studies reported here were performed with guinea pigs, a species for which the perception of infrasonic frequencies has never been measured. The ability to detect low frequencies has been correlated with cochlear length for species such as humans and guinea pigs with results showing that shorter cochleae are typically less sensitive to low frequencies (West, 1985; Echteler *et al.*, 1994). As compared to humans, guinea pigs require an average of 15 dB higher sound pressure level over the low-frequency range that has been measured (50–500 Hz; Heffner *et al.*, 1971; Miller and Murray, 1966; Prosen *et al.*, 1978; Walloch and Taylor-Spikes, 1976). We therefore expect guinea pigs to be less sensitive to infrasonic stimulation than humans and estimate the perceptual threshold for 5 Hz to be ~124 dB SPL. Thus responses to infrasonic frequencies are expected to be more robust in human cochleae than in guinea pigs.

In contrast to the IHCs, which are fluid coupled to the mechanical input, the stereocilia of the outer hair cells (OHCs) are directly coupled to the tectorial membrane, thus making OHCs sensitive to organ of Corti displacement (Dallos *et al.*, 1982; Dallos, 1986). Early studies by von Békésy (1951, 1960) showed that when the organ of Corti was displaced in a sustained manner by a mechanical probe, such as with a trapezoidal stimulus, the voltage response was sustained for the duration of the stimulus. These classic studies demonstrated that OHCs are capable of responding to very low frequencies. Salt and DeMott (1999) applied low-frequency stimulation by fluid injections into the perilymph and showed that large potentials, over 20 mV peak to peak (pk/pk) in amplitude, were generated in the endolymphatic space at stimulus frequencies from 10 Hz down to 0.1 Hz. Although stimulus delivery in this study was not by a normal, physiological route, responses of comparable magnitude were found during spontaneous middle-ear muscle contractions; this demonstrated that large potentials can indeed be elicited by physiologic stimuli. The amplitude of the cochlear microphonics (CMs) from stimuli in the range of audibility are typically less than ~2–3 mV pk/pk when measured in perilymph but have been shown to be up to ~8 mV pk/pk when recorded from the endolymph space of the apical cochlear turns (Honrubia and Ward, 1968; Honrubia *et al.*, 1973; Dallos, 1973). Salt *et al.* (2009) showed that

[a]Author to whom correspondence should be addressed. Electronic mail: salta@ent.wustl.edu

increases of endocochlear potential (EP) by more than 10 mV occurred when the organ of Corti was displaced toward scala tympani for a period of minutes by the slow injection of gel into the cochlear apex. These studies suggest that when the organ of Corti is displaced by low-frequency sounds, CM changes associated with OHC stimulation are greatest when recorded from the endolymphatic space.

In the present report, we examine the cochlear responses elicited by infrasonic and low-frequency acoustic stimulation. The issue of sensitivity to low-frequency sounds is becoming of greater importance because low-frequency environmental sounds are becoming more pervasive. People with wind turbines located near their homes can be exposed to low-frequency stimulation for prolonged periods of time (Jakobsen, 2005; van den Berg, 2006; O'Neal *et al*., 2011; Møller and Pedersen, 2011). Because infrasound is not heard, it is commonplace to high-pass filter the measured sounds with cutoff frequencies derived from the human audibility curve (A-weight) thereby diminishing low-frequency components (e.g., Møller and Pedersen, 2011). Other weighting functions give greater emphasis to infrasonic frequencies, such as G-weighting, which filters below 1 Hz and above 20 Hz at 24 dB/octave and emphasizes frequencies between 1 and 20 Hz according to their perceptual audibility (Broner, 2008). Wind turbines of contemporary design typically generate infrasonic levels of $\leq$70 dB G that are well below the 90 dB G level required for subjective hearing (Jakobsen, 2005; ISO, 1996). As infrasound levels from wind turbines are typically below the threshold of hearing, it has been widely concluded that the low-frequency components of the sound can be ignored. This has been encapsulated by the widely used quotation "What you can't hear, won't hurt you," which was attributed to an engineer named Campanella by Alves-Pereira and Castelo Branco (2007). Found elsewhere are numerous additional reports of wind-turbine noise assessments concluding that the infrasound level is insignificant because it is not heard (e.g., O'Neal *et al*., 2011). This particular subgenre of noise measurement and regulation is therefore almost entirely based on human *perception*. Our objective measures, such as those reported here, lead us to strongly advocate that before effects on humans can be dismissed, we must better understand the nature of the ear's response to infrasound in much greater detail.

II. METHODS

A. Animal preparation

This study used 13 guinea pigs under animal protocols 20070147 and 20100135 approved by the Animal Studies Committee of Washington University. Guinea pigs were initially anesthetized with 100 mg/kg sodium thiobutabarbital and maintained on 0.8%–1.2% isofluorane in oxygen. The trachea was cannulated, and the animal was artificially ventilated. End-tidal CO_2 was monitored with a capnograph (CapnoTrueAMP, Zevenaar, The Netherlands), and the tidal volume of the ventilator was adjusted to maintain an end-tidal CO_2 level of 5%. Body temperature was maintained at 38.5 °C with a DC-powered thermistor controlled heating pad. Pavulon (muscle relaxant) was given intravenously to suppress middle ear muscle contractions. The auditory bulla was exposed by a ventral approach and opened for the placement of recording electrodes.

B. Stimulus generation and delivery

Acoustic stimuli were delivered in a closed sound system. The external canal was sectioned and a hollow ear bar was inserted. An Etymotic Research ER-10 C acoustic assembly terminated near the tip of the earbar that also incorporated a Sennheiser HD 580 driver mounted in an acrylic coupler used to deliver low-frequency sounds. A probe tube to connect to a B&K 4134, [1/4]-in. reference microphone was also routed to the earbar. The B&K microphone was used to verify low-frequency calibrations, as it had a flat frequency response while the ER10C microphone incorporated low-frequency filtering.

Stimulus generation and data collection were performed with Tucker Davis System 3 hardware, driven by a custom written program (Microsoft Visual Basic) with ActiveX drivers. Three output channels were utilized, each routed though a Tucker Davis PA5 attenuator and Tucker Davis HB7 headphone amplifier. Sounds were calibrated in [1/4] octave steps from 4 Hz to 8 kHz for the Sennheiser transducer and 125 Hz to 22 kHz for the ER10C drivers.

C. Recording procedures

Most of the cochlear responses reported here were recorded through glass microelectrodes beveled to 4–6 μm tip outer diameter and filled with 500 mM KCl or 500 mM NaCl for endolymphatic and perilymphatic recordings, respectively. Electrodes were connected through Ag/AgCl wires and high input impedance ($>10^{14}$ Ω) DC-coupled amplifiers to the data acquisition system. The reference electrode was an Ag/AgCl pellet [RC1, World Precision Instruments (WPI), Sarasota, FL] connected though a fluid bridge to the muscles of the neck. In most cases, responses from endolymph and perilymph in the same cochlear turn were recorded simultaneously. Some responses (e.g., CAPs to high-frequency stimuli) were also recorded from an Ag/AgCl ball electrode placed on the edge of the round-window membrane near the bony annulus that was routed to a Tucker-Davis DB4 amplifier with the high-pass filter set at 5 Hz.

Four input channels of the Tucker-Davis system were sampled simultaneously, typically representing signals from the round window electrode, the ear canal microphone and two dc-coupled inputs from electrometers. An automated CAP audiogram was initially performed (1–22 kHz in [1/4] octave steps) to verify normal cochlear function. Measuring responses to low stimulus frequencies required collection windows of 4–6 s duration—a time consuming process when multiple response are averaged. Collection windows were therefore varied when measuring responses to stimuli of different frequency. For potential amplitude measurement algorithms, windows of 2 s, 200 ms, and 20 ms were used for frequencies below 25 Hz, from 25 to 250 Hz, and above 250 Hz, respectively. In most cases, dc-coupled responses were recorded. When responses to low-level stimuli were recorded for isopotential curves, band-pass filtering centered at the stimulus

frequency was used to reduce noise. At each frequency, a response average with no stimulus was performed to verify that the background noise was less than 60% of the criterion response amplitude of 100 μV.

D. Cochlear fluids manipulations

The sites of origin of cochlear responses were evaluated using an injection of isotonic KCl into perilymph at the apex to ablate sensory function progressively from apex to base. KCl solution was injected from a glass pipette coupled to a gas-tight syringe mounted on a digitally controlled pump (Ultrapump, WPI, Sarasota, FL). The pipette was sealed into the apex using established procedures that are documented elsewhere (Salt *et al.*, 2009). The mucosa covering the cochlear bone was removed at the apex, the bone was dried, and a thin layer of cyanoacrylate glue was applied that was covered with a thin layer of two-part silicone (Kwik-Cast, WPI, Sarasota, FL) to create a hydrophobic surface. A ~50 μm diameter fenestration was made through the adhesives and bone at the cochlear apex, and the tip of the injection pipette was inserted into perilymph. A tissue wick was used to remove the fluid droplet accumulating at the perforation site, and a drop of cyanoacrylate was immediately applied to seal the fenestration. Injection from a pipette sealed into the cochlea causes fluid flow to be directed toward the cochlear aqueduct at the basal turn of ST, displacing perilymph through the aqueduct into the ventricles. This results in an apical-to-basal progression of KCl that progressively ablates sensory cell function. Because the cross-sectional area of ST increases from apex to base, a constant injection rate would have caused the KCl front to slow as it approached the basal turn. We therefore progressively increased flow rate, from 50 nl/min (0–10 min), 100 nl/min (10–30 min), and 200 nl/min (≥30 min). The movement of KCl along the cochlea with this injection protocol was calculated using our established model of the cochlear fluids (available at http://oto.wustl.edu/cochlea/), which takes into account scala dimensions with distance, diffusion, flow rate, and communications with adjacent compartments.

E. Cochlear microphonic waveform analysis

To interpret CM response waveforms measured from endolymph, an analysis was performed in which the saturating response of the cochlear transducer was represented by a Boltzmann function driven by input sinusoids corresponding to the probe and bias stimuli. This approach is comparable to prior studies (Patuzzi and Moleirinho, 1998; Sirjani *et al.*, 2004; Brown *et al.*, 2009). The Boltzmann function used was similar to that described by Brown *et al.* (2009):

$$V_t = V_{EP} + (-V_{sat} + 2 \cdot V_{sat}/ (1 + \exp(-2 \cdot S_B/V_{sat}(P_t)))), \quad (1)$$

where V_{EP} is a DC potential representing the endocochlear potential magnitude (mV), V_{sat} is the saturation voltage of the Boltzmann curve (mV), S_B represents the slope of the Boltzmann curve at its mid-point (mV/Pa), P_t represents the input pressure (Pa) as a function of time.

Input to the function (P_t) was calculated as the sum of three independent inputs

$$P_t = P_{probe,t} + P_{bias,t} + OP,$$

where $P_{probe,t} = A_{probe} * \sin(2\pi f_{probe} t + \Phi_{probe})$ represents the probe tone (Pa) and $P_{bias,t} = A_{bias}/S * \sin(2\pi f_{bias} t + \Phi_{bias})$ represents the bias tone. OP represents the operating point of the transducer (Pa), defined as the pressure (i.e., the location on the Boltzmann curve) when probe and bias pressures are both zero. The variables A, f, and Φ define the amplitude, frequency and phase of the input tones respectively. S is a scale factor used to compensate for the difference in sensitivity to probe and bias tones at the specified sound pressure levels.

For some conditions, an additional sinusoidal potential at the frequency of the bias tone (f_{bias})was summed with the Boltzmann output as shown in Eq. (2).

$$V_t = V_{EP} + (-V_{sat} + 2 \cdot V_{sat}/ (1 + \exp(-2 \cdot S_B/V_{sat}(P_t)))) + V_o \cdot \sin(2\pi f_{bias} t + \Phi_{bias} + \Phi_o), \quad (2)$$

where V_o defines amplitude and Φ_o defines the phase of the potential relative to that of the bias tone Φ_{bias}. Calculated waveforms from Eqs. (1) and (2) were fitted to measured CM waveforms (5086 points) using the Solver add-in of Microsoft EXCEL. Best fit was established by minimizing the sum of squares of differences between measured and calculated waveforms.

III. RESULTS

A. Response amplitudes

Figure 1 shows an example recording from endolymph of the third turn of a guinea pig cochlea using a 5 Hz stimulus presented at 120 dB SPL. The pk/pk response amplitude was 19.1 mV—a sizable (23%) modulation of the resting EP that was 83.1 mV in this animal. The large amplitude of responses poses a scientific conundrum as 5 Hz presented at this level should be close to the subjective threshold, which we estimated earlier in Sec. I to be approximately 124 dB SPL in guinea pigs.

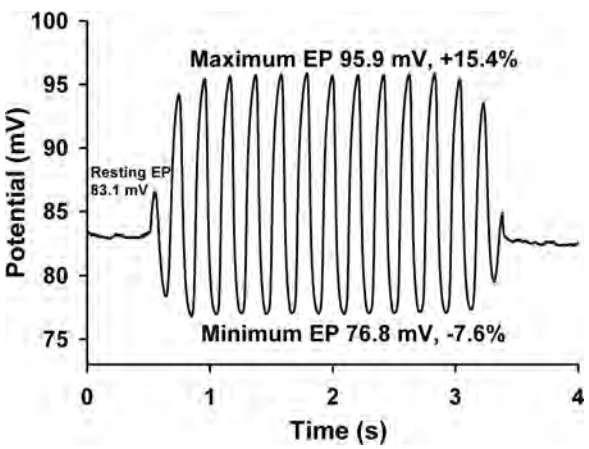

FIG. 1. Measured endolymphatic potential from cochlear turn 3 during stimulation with a single 5 Hz tone burst at 120 dB SPL. The sinusoidal potential represents a modulation of the normal (83.1 mV) endocochlear potential by over 20%.

CM response amplitudes (input/output functions) to low-frequency stimuli (5, 50, and 500 Hz) measured at four cochlear locations are summarized in Fig. 2. At each location, CM amplitudes exhibit the classic linear response with lower level stimuli and saturation with high level stimuli. In endolymph of turn 3 [Fig. 2(A)], although the response to 5 Hz at low levels (60 dB SPL, for example) was smaller than that to 50 or 500 Hz, the responses to 5 Hz at high levels did not saturate to the same degree as the higher frequencies such that the 5 Hz response was substantially larger (as indicated by the arrow). At the highest stimulus level tested (115 dB SPL) the peak amplitudes in endolymph of the third turn averaged 17.1 mV, and the largest individual responses were above 20 mV. These large responses to infrasound appear to be an apical endolymphatic phenomenon. Responses to 5 Hz were lower both in basal first turn endolymph [Fig. 2(B)] and in third turn perilymph [Fig. 2(C)]. Responses to 5 Hz were extremely small in first turn perilymph [Fig. 2(D)] and would likely be not detectable by conventional recordings from the round window membrane. The response amplitudes for infrasonic (5 Hz) stimuli in endolymph of the third turn were substantially larger than the maximum generated by tones in the normal range of audibility presented at any level.

The relative sensitivity across frequency from 5 to 1000 Hz measured as isoamplitude functions is shown in Fig. 3. In perilymph of the first and third cochlear turns, sensitivity decreased as frequency was lowered by approximately 7 and 10 dB/octave, respectively, from 500 to 50 Hz and 6 dB/octave for both turns between 50 and 5 Hz. In endolymph, the decline of sensitivity as frequency was lowered was less with slopes near 5 dB/octave from 500 to 5 Hz. The difference in sensitivity between endolymph and perilymph in each turn is shown in the lower panel of Fig. 3. The difference is in the 10–15 dB range around 500 Hz but increases progressively as frequency is lowered, so that endolymph measurements are 20–25 dB more sensitive than perilymph measurements in the 5–50 Hz range. This further demonstrates that responses measured from endolymph of the third turn to very low frequencies are far more sensitive than measured at other cochlear locations.

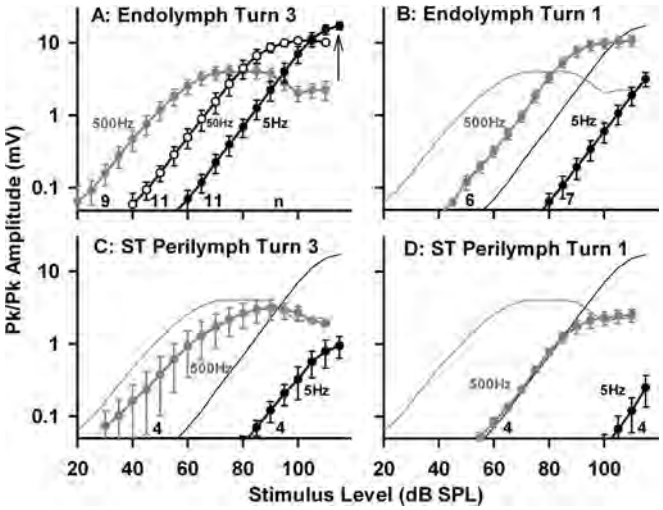

FIG. 2. Cochlear microphonic response amplitudes for 500 Hz (gray symbols), 50 Hz (open symbols), and 5 Hz (black symbols) stimulation recorded from four cochlear locations. Bars indicate s.d. Data for 50 Hz are only shown on (A) for clarity but were always intermediate between 5 and 500 Hz. Data from turn 3 endolymph are shown as thin lines on (B) through (D) for comparison. Responses from endolymph of turn 3 to 5 Hz were less sensitive than to 500 Hz at low stimulus levels but did not saturate to the same degree and markedly exceeded 500 Hz responses at high levels [indicated by the arrow on (A)]. Responses to 5 Hz were substantially lower in basal turn endolymph (B) and in third turn perilymph (C) and were almost absent from basal turn perilymph (D). At high stimulus levels, third turn endolymphatic potentials from infrasound (5 Hz, solid black symbols) were larger than for higher-frequency sounds presented at any level.

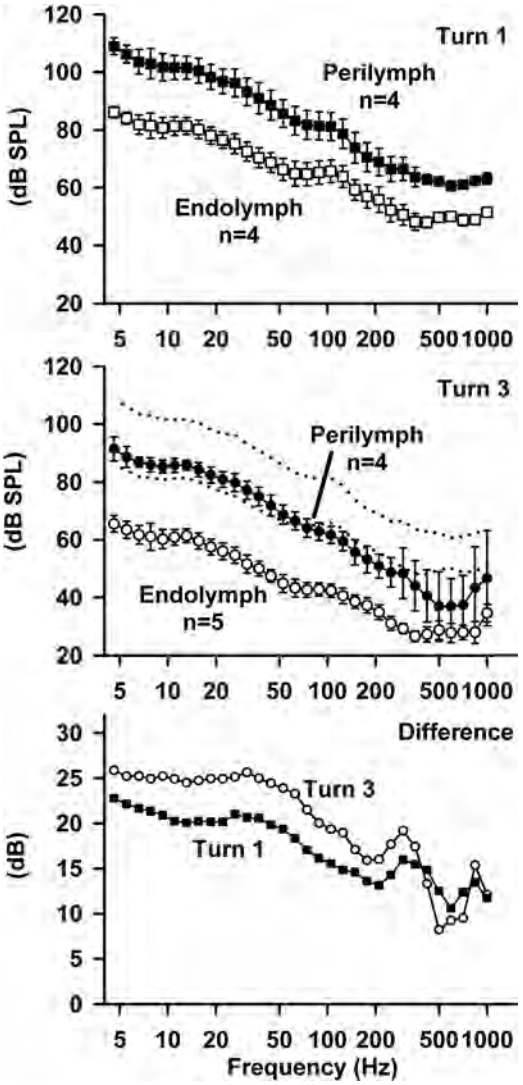

FIG. 3. Isopotential curves (100 μV) measured from 5 to 1000 Hz. Bars indicate s.d. Potentials were measured from endolymph (open symbols) and scala tympani perilymph (solid symbols) in cochlear turn 1 (top panel) and turn 3 (middle panel). At all probe-tone frequencies, a lower stimulus level was needed to evoke a 100 μV endolymphatic potential than for a perilymphatic potential. For comparison to cochlear turn 3 data, turn 1 data from the upper panel are shown as dotted lines in the middle panel (highest dotted line from perilymph and lowest dotted line from endolymph). Lower stimulus levels were needed to achieve a 100 μV turn 3 response in both scalae compared to turn 1. Turn 3 perilymph potentials from higher frequency probes were more variable due to higher background noise levels. The lower panel shows the mean endolymph-perilymph difference for the cochlear turns 1 and 3. The difference increased as frequency is lowered.

B. Origins of the large endolymphatic potentials

The origins of the large potentials recorded in endolymph were studied by injection of isotonic KCl from a pipette sealed into the cochlear apex. Injections into the sealed cochlea at rates 50 nl/min increasing to 200 nl/min result in a progressive apical to basal elevation of K^+ in ST; this ablates sensory cell function. The calculated K^+ concentration increases at different cochlear locations, based on the injection protocol used and guinea pig cochlear dimensions, are shown in the top panel of Fig. 4. The middle panel shows changes of EP and CM recorded from different locations, and the bottom panel shows CAP thresholds, each repeatedly measured through time during the injection in the same experiment. The CM to 4.8 and 238 Hz recorded from endolymph of turn 3 are the first responses to be affected by the injection. Around 17 min, the responses had both been reduced to less than 20% of the original amplitude—a decrease that occurred before CAP thresholds at any frequency had been affected. Responses recorded from the turn 1 electrode declined more slowly, consistent with their basal turn origins. CAP thresholds were progressively elevated in sequence from low to high frequencies, demonstrating the progressive and systematic dysfunction apex to base. EP magnitude from turns 1 and 3 declined more slowly than the sound-evoked potentials. These data, which were replicated in other experiments, demonstrate that the 5 Hz responses recorded from turn 3 endolymph have local origins in the apical regions of the cochlea.

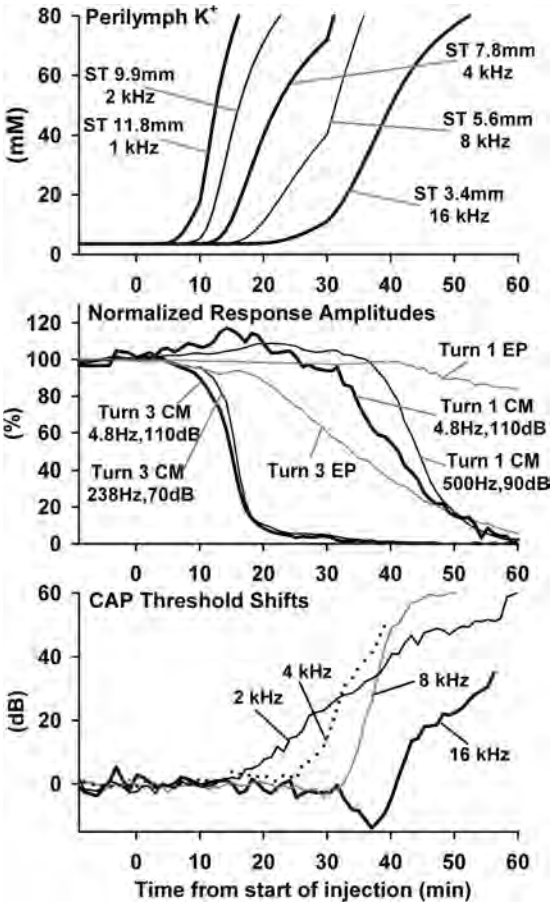

FIG. 4. Demonstration that third turn endolymphatic potentials are locally generated. Top: Calculated perilymph K^+ concentration increases at different locations along scala tympani (ST) resulting from the apical injection of KCl solution, starting at zero time. Labels indicate the distances along ST from the base in millimeters together with the best frequency of each location. The rate of injection increased with time so that the progression of KCl concentration increase occurred more uniformly even as the cross-sectional area of ST was increasing toward the base. Middle: Measured potentials from different cochlear locations repeated at 1 min intervals during the injection. All evoked potential measurements shown here were recorded in the same experiment. Responses from the third turn with 4.8 Hz, 110 dB SPL and 238 Hz, 70 dB SPL stimuli began decreasing after ~10 min while responses from turn 1 with 4.8 Hz, 110 dB SPL and 500 Hz, 90 dB SPL took much longer to decrease. The endocochlear potentials from the third and first turns declined more slowly than the sound induced responses. Bottom: Compound action potential (CAP) threshold shifts recorded at the round window at specific tone-burst frequencies as indicated. CAP thresholds increased sequentially from low to high frequencies as the KCl solution progressively moved down the cochlea with time. The 4.8 Hz response recorded from turn 3 (middle panel) was substantially reduced before the 2 kHz CAP—the lowest CAP tone-burst frequency—threshold was elevated, clearly showing that it was generated from an apical region.

C. Infrasound biasing studies

The existence of potentials generated locally in the third turn with amplitudes larger than the voltage at which CM saturates with higher frequency stimuli led us to consider how such large potentials could be generated by cochlear transduction. We studied this by combining a probe tone that saturated the transducer with an infrasonic bias tone that would normally generate responses of large amplitude. In previous biasing studies, the focus has typically been on how slow displacements of the sensory structures caused by bias tones influence responses to higher-frequency probe stimuli. The present study differs in that we wanted to understand the influence of probe tones on response to bias tones to study the origins in the infrasonic responses For this purpose, we needed a probe tone to partially saturate mechanoelectric transduction to define the transducer characteristics. However, probe tones at the required levels strongly suppressed the response to infrasonic bias tones. Figure 5 shows a paradigm in which a 500 Hz probe tone was superimposed on a 4.8 Hz infrasonic bias tone. As the level of the 500 Hz tone was increased, the response to 4.8 Hz was strongly suppressed. Suppression of bias responses has been reported elsewhere (Cheatham and Dallos, 1982, 1994). The response amplitude during the 4.8 Hz-alone segment (Infra Alone) was measured as the amplitude of a 4.8 Hz sinusoid that was best fit to the CM. The response amplitudes to both the probe and bias components when both were presented simultaneously were measured by fitting the sum of a 4.8 Hz sinusoid and a 500 Hz sinusoid passed through a Boltzmann function (representing the saturating response to the probe). This allowed both bias- and probe-response amplitudes to be independently quantified, as shown in the middle panel. It is apparent that the response to the infrasonic tone in the presence of the probe [Fig. 5(B) labeled "Infra + (probe)"] was suppressed at probe levels as low as 65 dB SPL, which is well below the 80–85 dB SPL where saturation of the probe occurs [Fig. 5(B) labeled "Probe + (infra)"]. However, the suppression was caused by the saturation associated with the response to the probe as shown in Figs. 5(C) and 5(D). In Fig. 5(C), the amplitude of the response to the probe was compared with a linear, theoretical

response in which response amplitude increases by 1 dB/dB. Deviations from this line became progressively greater as the probe level increased and responses became saturated. This shows that saturation starts occurring at probe levels well below those that produce maximum response amplitude. In Fig. 5(D), the response to infrasound was multiplied by the ratio of the probe response to the theoretical line, thus scaling the infrasound response to the same extent as the probe response saturates. The calculated curve [Fig. 5(D), dark solid line] closely matched the measured reduction of infrasound responses with increasing probe level, suggesting that physiological processes associated with saturation of the probe accounted for the suppression of the infrasound response.

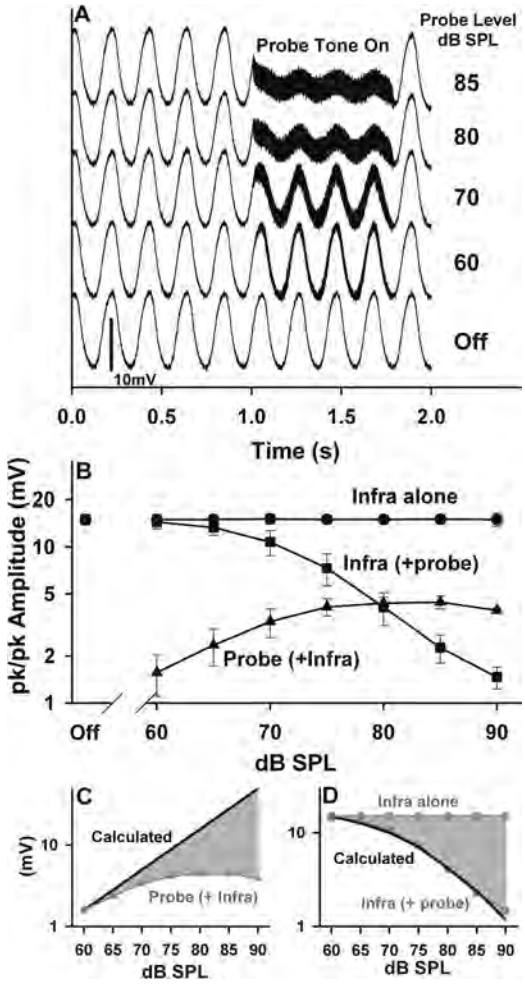

FIG. 5. (A) Influence of a 500 Hz probe tone added to an infrasonic (infra) stimulus (4.8 Hz, 110 dB SPL). Endolymphatic potentials were recorded from the third turn as a single epoch with no averaging. As the level of the probe tone increased, the response to infrasound was strongly suppressed. (B) Measured response amplitudes averaged in three animals. Bars indicate s.d. "Infra alone" indicates the amplitude of the infrasound response when presented alone. "Infra(+probe)" indicates the amplitude of the infrasound response when the probe was simultaneously on. "Probe(+infra)" indicates the amplitude of the probe response measured with the infrasound simultaneously on. (C) The measured response to the probe is compared with a linear (1 dB/dB) function. (D) The calculated curve shows the response to the infrasound tone alone corrected for the amplitude ratio of the probe relative to the calculated line from (C). The calculated curve closely fits the measured infrasound amplitude with the probe on. This demonstrates that the suppression of the infrasonic response arose from probe-tone-induced changes in the mechanoelectric transducer function.

An analysis of CM responses to infrasound in the presence of probe tones therefore needed to consider the suppression of the infrasound response by the probe at levels that even partially saturated the transducer. We were primarily interested in the origins of the large infrasound responses in the absence of a probe. Responses were therefore initially measured at a constant level of infrasound as the probe tone was varied in level. dc-coupled CM measurements from endolymph of the third turn with a fixed-level infrasonic bias tone (4.8 Hz, 110 dB SPL) and varied level of 238 Hz stimulation are illustrated in Fig. 6. Responses averaged to 10 bias-tone cycles are displayed as a single bias cycle. At low probe levels, the response to 238 Hz was highly modulated but as probe level was increased the degree of modulation decreased and the amplitude of the response to the 4.8 Hz bias tone was reduced. A notable feature in these recordings is that the regions where there was most saturation of the probe tone—indicated by asterisks on the 75 dB SPL trace—did not coincide with the times of minimum or maximal potential produced by the bias. This was a consistent finding in all animals tested. This means that the greatest influence of biasing on the probe response did not coincide in time with the largest bias-induced endolymphatic potentials.

A theoretical calculation showing the output from a saturating transducer represented by a first-order Boltzmann curve [Eq. (1)] in response to combined probe-plus-bias input stimuli is shown in Fig. 7. An asymmetry between the calculated output during negative and positive bias half-cycles, as seen in the experimental data, was produced by setting the operating point to a non-zero value [indicated by the black circle on Fig. 7(B)]. The operating point represents the resting position on the curve with no stimulus present. With a Boltzmann function of this type, the maximum and minimum voltages to

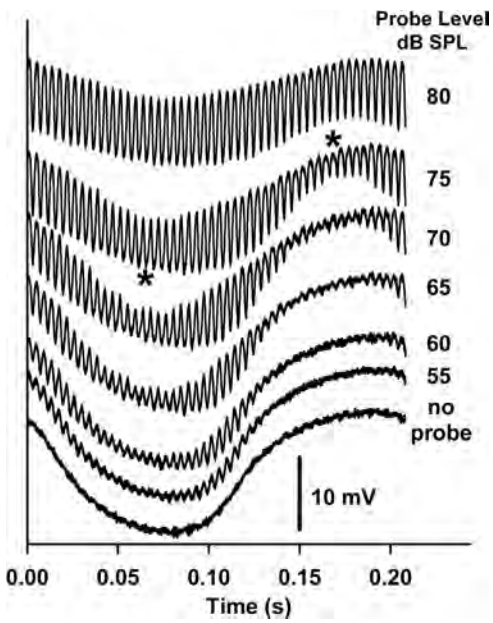

FIG. 6. Responses measured from the endolymphatic space of the third turn with a 4.8 Hz bias tone at 110 dB SPL and a 238 Hz probe tone that was varied in level. Responses are shown for a single cycle of the bias tone. As the probe level increased, the degree of modulation of the probe and the response amplitude to the bias both decreased. Additionally, the time when there was maximum saturation of the probe-tone response (asterisks) did not coincide with the times of maximum or minimum voltage generated by the bias.

the bias tone occur when the probe response is displaced at extremes of the curve and cause maximum saturation of the probe response. Single probe-tone cycles at extreme displacements are shown as dark thin lines on Fig. 7(C). This analysis did not provide a good representation of the measured responses from endolymph.

A solution that better represented the measured data was provided by a modification of the analysis in which a separate bias-generated sinusoidal potential was summed with the Boltzmann output, as represented in Eq. (2). This approach was initially justified by prior observations that tone-induced responses in endolymph could be offset by many millivolts during gel injections into the cochlear apex causing sustained displacements of the organ of Corti (Salt *et al*., 2009). Adding a phase-delayed potential at the bias frequency to the model allowed it to closely fit the measured CM waveforms as shown in Fig. 8. Figure 8(A) shows a CM waveform (from Fig. 6; probe level 75 dB SPL). Figure 8(B) shows the measured and calculated waveforms superimposed, and Fig. 8(C) shows the calculated waveform alone. Figure 8(D) shows individual components as a function of time, and Fig. 8(E) shows the same components plotted as a function of input pressure (i.e., as a transducer function). In both of these panels, the gray curves show the Boltzmann output to the combined probe-plus-bias. Panels (D) and (E) show that in addition to modulating the probe-tone response, bias-induced displacements also produce a potential change, as previously shown by the analysis presented in Fig. 7. This can be considered as the bias moving operating point up and down the Boltzmann curve, generating the potential change V_B (i.e., the voltage predicted from the Boltzmann curve), which is shown as a dotted line on both panels. The dashed line, appearing as an ellipse in Fig. 8(E) shows the additional potential V_o from Eq. (2), in this case delayed in phase by 40° with respect to the mechanical effects of the bias. This analysis suggests that the large low-frequency potentials recorded in endolymph may be accounted for by additional components that are not directly generated by the saturating transducer that the Boltzmann curve represents. The same analysis was not possible with data recorded from perilymph due to the far smaller 4.8 Hz response component in the measurement.

A summary of the most relevant parameters derived from the Boltzmann-plus-V_o [i.e., Eq. (2)] analysis of CM from the first and third cochlear turns are presented in Fig. 9. In the third turn, parameters were more dependent on probe level than in the basal turn due to the lower levels required to cause response saturation by the probe. The V_o component in the third turn was smaller than V_B with mean ratios varying from 0.3 (90 dB probe) to 0.7 (75 dB probe). This means that in the third turn, a potential with amplitude of approximately half that generated by the transducer's response to the bias may be present in the CM. In contrast, V_o was lower in the basal turn, but V_B was far lower there, so mean ratios varied from 0.3 (95 dB probe) to 2.4 (75 dB probe). Waveforms to the lower probe levels and to the no-probe condition were fitted by holding the parameters for the probe- and the bias-offset phase constant at values established with higher-level probes, showing that results with the bias alone were generally consistent with those at low-probe levels. In experiments where bias levels were varied holding probe tone level constant (Fig. 9, bottom row), both V_B and V_o components varied in a near-linear manner for both the apical and basal turns with ratios that were relatively uniform across bias level. The ratios were similar in the basal and third turns just by chance based on the choice of probe levels used as seen in the top panel. The slope parameter S_B is also

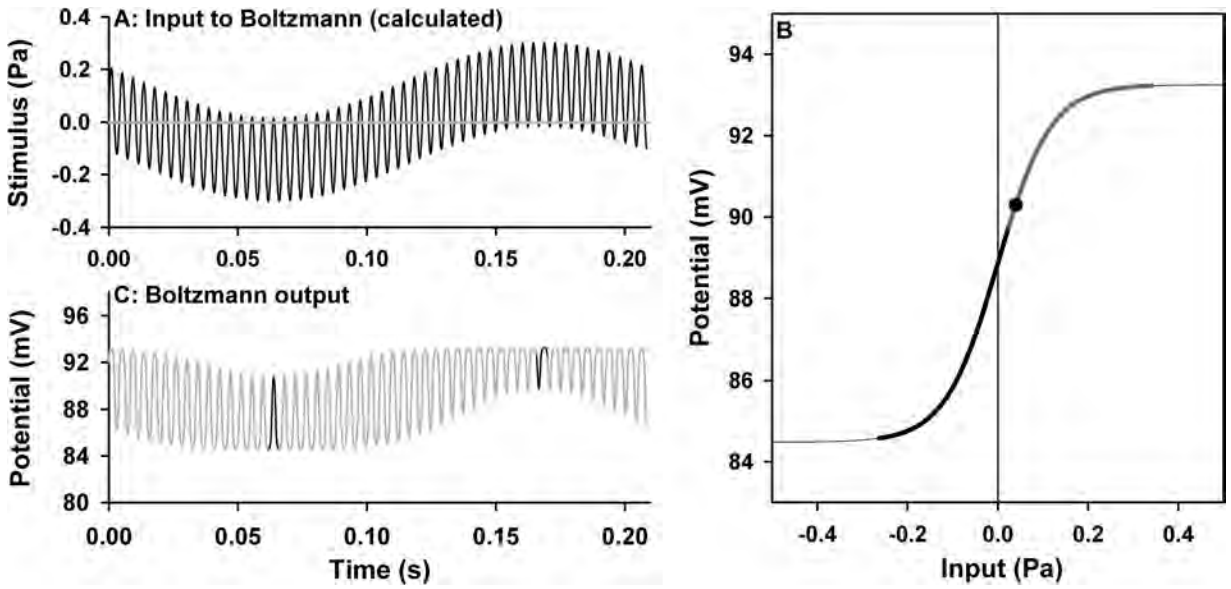

FIG. 7. (A) Combined infrasound bias plus probe stimulus combination that was the input for the calculation. The input is shown for a single cycle of the bias tone. (B) First-order Boltzmann curve relating output potential (y) to input pressure (x). A non zero operating point (black dot) is summed with the input to introduce asymmetry into the output waveform. (C) Calculated output from the Boltzmann function showing an asymmetric modulation as seen in the physiologically measured responses in Fig. 6. However, unlike the physiologically measured responses, the maximum and minimum potential from the low-frequency bias tone always coincided with the maximum degree of saturation of the probe response. This shows that a simple Boltzmann analysis cannot account for the measured response waveforms. Single cycles of the probe tone at the negative and positive limits of the bias tone are shown in (C) and are represented by the heavy gray and black lines on the curve in (B).

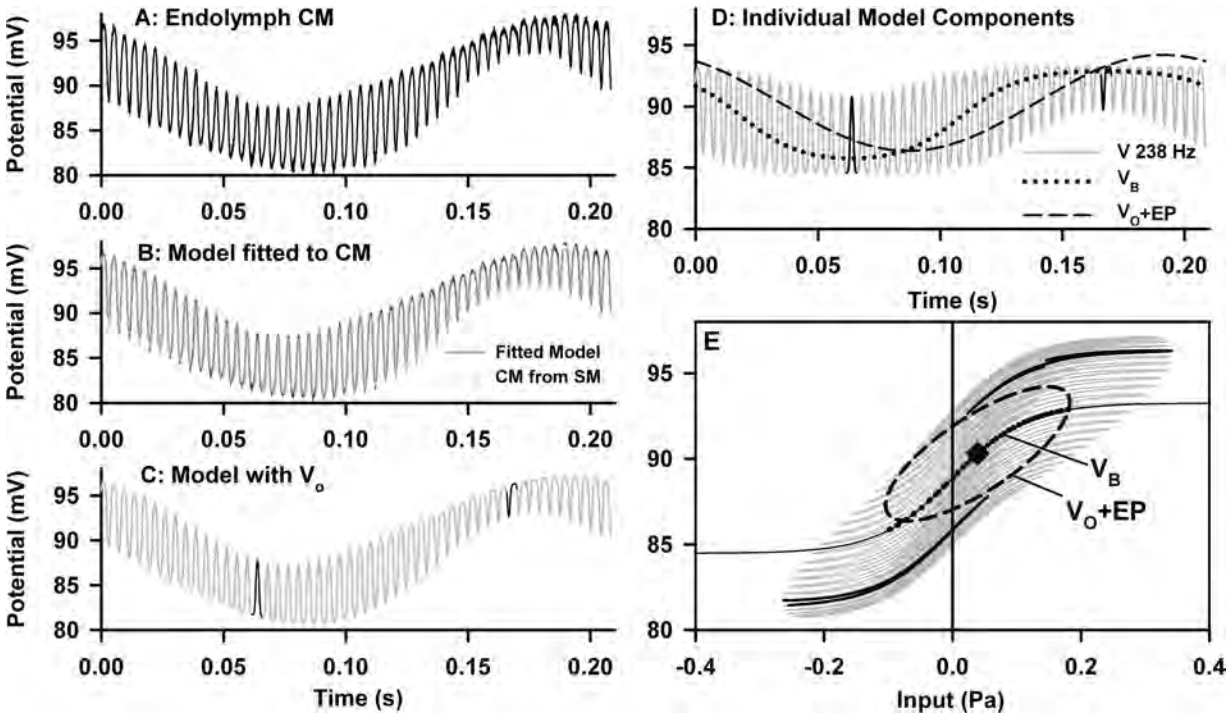

FIG. 8. Simulation in which a phase-delayed sinusoidal "offset" component (V_o) is summed with the Boltzmann output to represent the measured waveforms. (A) Physiologic data (the trace from Fig. 6 at the 75 dB probe level). (B) Calculated and measured curves overlaid showing that the analysis closely represents the measured waveform. (C) Calculated output curve with two individual cycles of the probe shown at the minimum and maximum bias pressures. (D) Components of the model, with the Boltzmann output show in gray and the phase-delayed offset component (V_o) shown dashed. A constant voltage (the EP value at the operating point) has been added to so it can be displayed in the figure. In this example, the phase delay was −40 deg. The dotted line shows the output voltage change from the bias tone displacing operating point on the Boltzmann curve (V_B). (E) Input/output relationship shown as a Boltzmann curve (thin black line) with added potential V_o + EP (dashed circle) that produces the overall the output waveform (gray lines). Single cycles of the probe at the minimum and maximum bias pressures are shown in black. The dotted line labeled V_B shows the voltage change caused by the bias tone displacing the operating point (black diamond) on the curve. This simulation illustrates that the salient characteristics of the physiologically measured waveforms are represented by this analysis.

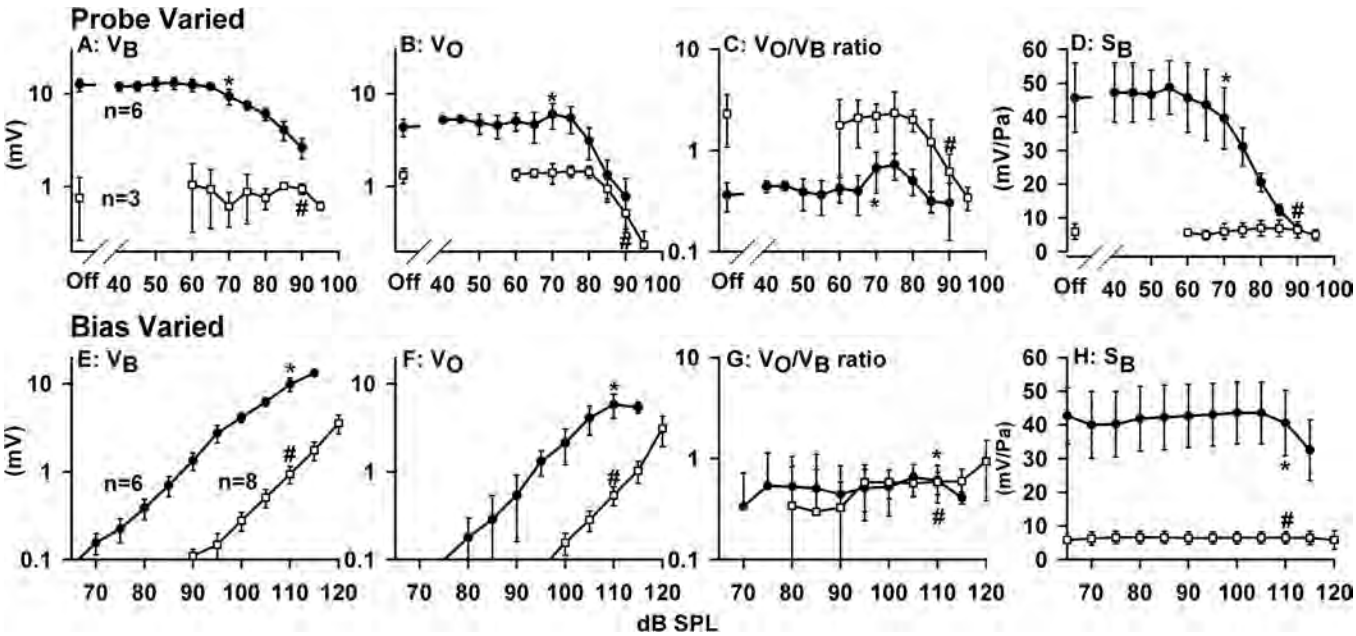

FIG. 9. Parameters derived from analysis of response waveforms recorded from the basal turn (open symbols, probe stimulus 476 Hz) and from the third turn (solid symbols, probe stimulus 238 Hz); When the probe was varied (top row), the bias level was fixed at 110 dB SPL. When the bias was varied (bottom row) the probe was set to 70 dB SPL (third turn) and 90 dB SPL (basal turn). In each row, the potential generated by the bias displacing operating point on the Boltzmann curve (V_B), the offset component (V_o) and their ratio under each condition are shown. Also shown in (D) and (H) are values of the slope parameter, S_B, that remained nearly constant for basal turn data but fell markedly as probe level was increased above 55 dB SPL for third turn data. The labels * and # represent those conditions that were replicated in both series. The number of experiments in each condition are shown on (A) and (E).

TABLE I. Average parameters derived from Boltzmann–plus-V_o waveform analysis.

	V_o phase (deg)	Bias correction (dB)	Operating point (Pa)	P_{sat} (mV)	N
		Probe varied			
Turn 3	−58.2	−33.51	0.007	5.99	38
	SD 18.0	SD 2.9	SD 0.042	SD 1.23	
Turn 1	−73.6	−42.27	−0.108	4.17	17
	SD 16.9	SD 2.7	SD 0.114	SD 0.76	
		Bias varied			
Turn 3	−61.64	−34.4	−0.002	6.11	47
	SD 22.0	SD 3.3	SD 0.02	SD 1.31	
Turn 1	−60.68	−41.02	−0.007	4.17	59
	SD 10.2	SD 3.38	SD 0.089	SD 0.53	

shown to change markedly in the third turn at higher probe levels and at the highest bias levels, while it was near constant for basal-turn data. The remaining parameters that did not vary systematically with level are shown averaged in Table I. Low probe levels (with probe varied) and low-bias levels (with bias varied) were excluded from the summary. The phase of V_o with respect to V_B averaged approximately −60 deg and was relatively consistent across all animals tested. The average bias scaling factor (S) derived from the analysis, shown in Table I in decibels, was approximately −34 dB for the third turn and −42 dB for the basal turn. These factors were derived from the waveform fitting procedure based on the amount of bias-induced displacement that accounted for the waveform shape of the response to the probe. The values were also consistent across animals and were comparable to differences in sensitivity across frequency shown for the two locations in Fig. 3.

IV. DISCUSSION

This study demonstrated that infrasound elicits larger electrical potentials in the apical regions of the cochlea than those generated by any other frequencies in the range of audibility. This confirms the existence of large endolymphatic responses seen in prior studies with low-frequency stimulation from 0.1 to 10 Hz (Salt and DeMott, 1999), although in this present study with sounds delivered acoustically via the external ear canal. The apical regions of the cochlea should therefore be regarded as highly responsive to infrasound stimulation with responses occurring at stimulus levels well below the estimated level that is perceived.

The large potentials recorded from endolymph of the third turn are locally generated and are not generated at some distant site such as the saccule. This is demonstrated by the rapid loss of responses recorded from cochlear turn 3 as KCl solution was injected at the apex. Responses to infrasound undoubtedly originate from stimulation of the OHC but are enhanced in a manner that we have quantified as an additional voltage component (V_o). CM measurements can be difficult to interpret as they are vectorally summed voltages from different regions, weighted with distance from the recording site. Gross CM measures typically do not reflect cochlear amplification because rapid frequency-dependent phase changes near the best frequency of a tone produce opposing voltages that cancel and so are not represented in the measurement (Whitfield and Ross, 1965; Cheatham and Dallos, 1982). The picture becomes simplified for CM to stimulation below the best frequency of the recording site. Phase-frequency changes are less rapid presumably because broader regions of the basilar membrane vibrate with similar phase. Phase-frequency changes are expected to be similar for infrasonic stimuli. The KCl ablation experiments (Fig. 4) show that the sites of origin of the infrasound and probe responses are similar, especially for the third turn responses. As both the infrasonic and probe stimuli are well below the best frequency of our recording site, which for the cochlear turn 3 recording site corresponds to ∼1 kHz, responses likely arise from passive cochlear mechanics.

There are a limited number of mechanisms that may give rise to V_o. If V_o arose as a dc component in the bodies of the OHCs, rather than at the mechanoelectrical transducer (MET), it would be seen in the endolymph through the resistance of the MET channels and modulated by both the probe and bias accordingly. A dc component in the OHC bodies can therefore be excluded. The IHC are also an unlikely source of V_o. Cheatham and Dallos (1994) reported that IHC dc responses were only minimally affected by a 20 Hz tone presented alone. In our measures, we found the difference between endolymph and perilymph responses increased as frequency was lowered; this is not consistent with decreasing IHC sensitivity for lower frequencies. The observation that sustained displacements of the organ of Corti by gel injection at the apex yielded V_o-like potentials when velocity and IHC stimulation would be negligible also argues against an IHC origin (Salt *et al.*, 2009). If the OHC and IHC are not the source of V_o, this leads to the possibility that non-sensory tissues of the inner ear may be contributing to the endolymphatic potentials. One possibility is that when under increased or decreased current load for a long duration, as in each half-cycle of an infrasonic stimulus, ion transport processes in the lateral wall generating EP are affected. This is comparable to a high current load on a battery causing the voltage to fall and a reduction in current load causing the voltage to rise. The possibility of changes in current drawn by the hair cells altering K^+ levels in the intrastrial space, thereby causing greater EP changes was considered in a model of EP generation (Quraishi and Raphael, 2008). Indeed, the use of low-frequency or sustained displacements of the organ of Corti to change potential in endolymph may provide a tool to evaluate the current generation capacity of stria vascularis, analogous to testing a battery by applying a high current load. This putative mechanism accounts for both the data presented here and for the large EP changes when the organ of Corti was displaced by gel injections into the apex (Salt *et al.*, 2009). Nevertheless, there may be alternative explanations if other stimulation modes of either IHCs or OHCs occur at infrasonic frequencies (Nowotny and Gummer, 2006; Guinan, 2012) or if significant potential can be generated by ion transport at other loci in the endolymphatic boundary.

The saturation, and subsequent decline, of CM growth functions with stimulus level increases (Fig. 2) has been

well-documented in classical studies although the mechanism underlying the phenomenon has not been well-described. The saturation is partly accounted for by the response characteristic of OHC that is sigmoidal and saturating with sinusoidal input. The limits of the saturating characteristics to extreme displacements represent all–channels-open and all-channels-closed—saturated states but do not explain the subsequent response decline as stimulus levels are further increased. In our analysis of waveforms, the saturating response characteristic of the Boltzmann curve is taken into account, and amplitude changes that are not accounted for by saturation are represented in the slope parameter S_B. In the fixed-bias-plus-varying-probe paradigm with low-level 238 Hz probe stimuli, S_B for third turn measurements averaged ~48 mV/Pa but declined progressively for probe levels of 60 dB and higher [Fig. 8(D)]. In contrast, in the fixed-probe-plus-varying-bias paradigm S_B was quite insensitive to the infrasonic bias level, declining only at the highest probe levels [Fig. 8(H)]. This leads us to conclude that in the absence of a probe stimulus, the endolymphatic potential in response to infrasound remains large and does not saturate because the sensitivity S_B remains high. In contrast, when a high level probe is added, S_B is reduced, which influences response amplitudes from both the probe and the bias tones. This is reflected in the suppression of the bias tone in Fig. 5 as the probe tone level is increased with the decline in bias response being accounted for by the reduction in sensitivity caused by the probe. S_B may be reduced by mechanical or electrical influences. Cooper and Rhode (1995) reported substantial two-tone suppression on the low-frequency side of the best frequency in apical mechanical measures in their study that focused quantifying the effects of a low-frequency bias tone on a higher-frequency probe rather than the effects of higher frequencies on the low-frequency bias response. In our study, one can think of this effect as the sensitivity to infrasound stimulation being maximal unless frequencies within the range of audibility are present at sufficient level to decrease the sensitivity of the *in vivo* transducer.

The endolymphatic potentials evoked by infrasound that we reported here were made through dc-coupled instrumentation and would not be detected with extracochlear recordings, such as from an electrode near the round window membrane. The response magnitude from perilymphatic sites was shown to be substantially lower and the high-pass filtering and ac coupling typically employed in extracochlear recordings would attenuate the responses further.

The EP plays a pivotal role as the battery for cochlear transduction, providing a substantial part of the electrochemical voltage driving current through the transduction channels of the hair cells. Small EP changes have been shown to substantially influence auditory sensitivity at high frequencies. A classic study by Sewell (1984) found that auditory sensitivity in cats was elevated by ~1 dB for every ~1 mV decrease in EP. Schmiedt *et al.* (2002) found a similar relationship in aged and furosemide-treated gerbil cochleae although they found far less dependence of low-frequency sensitivity on EP in higher turns that they attributed to there being less cochlear amplifier gain for low-frequency sounds. The EP changes we observed with infrasound would be expected to modulate cochlear amplifier gain for tones at their best frequency region, which would be perceived as an amplitude modulation of the tone. Biasing studies suggest the IHC respond to extracellular potentials generated by very low-frequency tones presented at high levels (Cheatham and Dallos, 1997), but the degree of sensitivity of IHC to EP and other extracellular responses to infrasonic tones (i.e., the infrasound levels at which IHC stimulation occurs) remains unknown. Objective physiologic measures of responses to low-frequency and infrasonic stimulation are not readily available. CAPs utilize onset synchrony are not sensitive indicators of low-frequency neural function but new methods, utilizing phase synchrony of low-characteristic frequency single-auditory-nerve-fibers, are becoming available to quantify apical function (Lichtenhan *et al.*, 2012). These new techniques will allow infrasound-induced modulation of neural function to be measured and compared with EP changes.

We previously estimated that with low-frequency stimulation the OHC can respond at levels as low as 40 dB below the sensitivity of the IHC; i.e., 40 dB below the threshold of hearing (Salt and Hullar, 2010). Based on the measurements in the current study, the 40 dB figure could have been an underestimate because here we have found that the apical regions of the ear are more sensitive to infrasound than we previously appreciated. We found responses to infrasound levels as low as 60–65 dB SPL (Figs. 2 and 3), in part due to the enhancement of infrasonic responses in the endolymphatic space relative to the perilymphatic space. Comparing endolymphatic potentials with hearing thresholds in guinea pigs requires consideration of the experimental conditions under which they are made. The measures were made with the auditory bulla open, the effects of which are shown to be uniform across frequency below 300 Hz but increase sensitivity by 10–15 dB (Manley and Johnstone, 1974; Wilson and Johnstone, 1975). When frequency-dependent sensitivity is considered, we would estimate that free field simulation of 70–80 dB SPL (i.e., 44–54 dB below hearing threshold) is stimulating the cochlear apical regions of the guinea pig to a degree where a 100 μV response amplitude is generated. If the human cochlea is about 15 dB more sensitive than the guinea pig, we estimate that apical regions of the human could be stimulated with 5 Hz stimulation at 55–65 dB SPL, which corresponds to −38 to −28 dBA. This estimate awaits some form of direct experimental confirmation in humans.

There is currently intense debate over whether infrasound exposure can influence human health. As wind turbines have become larger in recent years, they generate higher levels of low-frequency noise and infrasound (Møller and Pedersen, 2011). Some people who live near wind turbines report being sickened with symptoms that resolve when they move away. The wind industry generally dismisses such reports on basis that humans cannot be affected by sounds that are not heard. The present studies show that the cochlear apex is highly sensitive to low-frequency stimulation. The potentials we observed are initiated by the OHC and enhanced in the endolymphatic space by additional mechanisms, making them larger than responses to stimuli within the range of audibility. The degree of IHC stimulation caused by the changes in endolymphatic potentials remains uncertain. A scientific conundrum remains

over why the cochlea would transduce such sounds and generate large potentials and then discard this information from conscious hearing. The answer may be that the majority of low-frequency sound is unwanted noise, such as from respiration, heartbeat, head movements, etc. There may be mechanisms present both to transduce the sound and then cancel it from conscious hearing (analogous to a noise-canceling headphone). Neural pathways exist from the OHC to the cochlear nucleus, which are potentially inhibitory to hearing (Kaltenbach and Godfrey, 2008) and could suppress perception of responses mediated by the IHC. Although there is clearly a need to understand how the ear responds to low-frequency sounds in more detail and how it affects the body as a whole, the present study confirms that the inner ear is highly sensitive to infrasonic and low-frequency stimulation. It seems unreasonable to believe that infrasound cannot influence the animal or person when it generates such large endolymphatic potentials.

Alves-Pereira, M., and Castelo Branco, N. A. (**2007**). "Vibroacoustic disease: Biological effects of infrasound and low-frequency noise explained by mechanotransduction cellular signaling," Prog. Biophys. Mol. Biol. **93**, 256–279.

Broner, N. (**2008**). "Effects of infrasound, low-frequency noise and ultrasound on people," in *Handbook of Noise and Vibration Control*, edited by M. J. Crocker (Wiley and Sons, Hoboken, NJ), pp. 320–325.

Brown, D. J., Hartsock, J. J., Gill, R. M., Fitzgerald, H. E., and Salt, A. N. (**2009**). "Estimating the operating point of the cochlear transducer using low-frequency biased distortion products," J. Acoust. Soc. Am. **125**, 2129–2145.

Cheatham, M. A., and Dallos, P. (**1982**). "Two-tone interactions in the cochlear microphonic," Hear. Res. **8**, 29–48.

Cheatham, M. A., and Dallos, P. (**1994**). "Stimulus biasing: A comparison between cochlear hair cell and organ of Corti response patterns," Hear. Res. **75**, 103–113.

Cheatham, M. A., and Dallos, P. (**1997**). "Low-frequency modulation of inner hair cell and organ of Corti responses in the guinea pig cochlea," Hear. Res. **108**, 191–212.

Cheatham, M. A., and Dallos, P. (**2001**). "Inner hair cell response patterns: Implications for low-frequency hearing," J. Acoust. Soc. Am. **110**, 2034–2044.

Cooper, N. P., and Rhode, W. S. (**1995**). "Nonlinear mechanics at the apex of the guinea-pig cochlea," Hear. Res. **82**, 225–243.

Dallos, P. (**1970**). "Low-frequency auditory characteristics: Species dependence," J. Acoust. Soc. Am. **48**, 489–499.

Dallos, P. (**1973**). *The Auditory Periphery* (Academic, New York), pp. 228–246.

Dallos, P. (**1986**). "Neurobiology if cochlear inner and outer hair cells: Intracellular recordings," Hear. Res. **22**, 185–198.

Dallos, P., Santos-Sacchi, J., and Flock, Å. (**1982**). "Intracellular recordings from cochlear outer hair cells," Science **218**, 582–584.

Echteler, S. M., Fay, R. R., and Popper, A. N. (**1994**). "The influence of cochlear shape on low frequency hearing," in *Comparative Hearing: Mammals*, edited by R. R. Fay and A. N. Popper (Springer, New York), pp. 134–171.

Franke, R., and Dancer, A. (**1982**). "Cochlear mechanisms at low frequencies in the guinea pig," Arch. Otorhinolaryngol. **234**, 213–218.

Guinan, J. J., Jr. (**2012**). "How are inner hair cells stimulated? Evidence for multiple mechanical drives," Hear. Res. **292**, 35–50.

Heffner, R., Heffner, H., and Masterton, B. (**1971**). "Behavioral measurements of absolute and frequency-difference thresholds in guinea pig," J. Acoust. Soc. Am. **49**, 1888–1895.

Honrubia, V., Strelioff, D., and Ward, P. H. (**1973**). "A quantitative study of cochlear potentials along the scala media of the guinea pig," J. Acoust. Soc. Am. **54**, 600–609.

Honrubia, V., and Ward, P. H. (**1968**). "Longitudinal distribution of the cochlear microphonics inside the cochlear duct (guinea pig)," J. Acoust. Soc. Am. **44**, 951–958.

ISO (**1996**). 7196, *Acoustics—Frequency-Weighting Characteristic for Infrasound Measurements* (International Organization for Standardization, Geneva, Switzerland).

Jakobsen, J. (**2005**). "Infrasound emission from wind turbines," J. Low Freq. Noise Vib. Active Control **24**, 145–155.

Kaltenbach, J. A., and Godfrey, D. A. (**2008**). "Dorsal cochlear nucleus hyperactivity and tinnitus: Are they related?," Am. J. Audiol. **17**, S148–S161.

Lichtenhan, J. T., Cooper, N. P., and Guinan, J. J. (**2012**). "A new auditory threshold estimation technique for low frequencies: Proof of concept," Ear Hear. **34**, 42–51.

Manley, G. A., and Johnstone, B. M. (**1974**). "Middle-ear function in the guinea pig," J. Acoust. Soc. Am. **56**, 571–576.

Miller, J. D., and Murray, F. S. (**1966**). "Guinea pig's immobility response to sound: Threshold and habituation," J. Comp. Physiol. Psychol. **61**, 227–233.

Møller, H., and Pederson, C. S. (**2004**). "Hearing at low and infrasonic frequencies," Noise Health **6**, 37–57.

Møller, H., and Pedersen, C. S. (**2011**). "Low-frequency noise from large wind turbines," J. Acoust. Soc. Am. **129**, 3727–3744.

Nowotny, M., and Gummer, A. W. (**2006**). "Nanomechanics of the subtectorial space caused by electromechanics of cochlear outer hair cells," Proc. Natl. Acad. Sci. USA **103**, 2120–2125.

O'Neal, R. D., Hellweg, R. D., Jr., and Lampeter, R.M. (**2011**). "Low frequency noise and infrasound from wind turbines," Noise Control Eng. J. **59**, 135–157.

Patuzzi, R., and Moleirinho, A. (**1998**). "Automatic monitoring of mechano-electrical transduction in the guinea pig cochlea," Hear. Res. **125**, 1–16.

Prosen, C. A., Petersen, M. R., Moody, D. B., and Stebbins, W. C. (**1978**). "Auditory thresholds and kanamycin-induced hearing loss in the guinea pig assessed by a positive reinforcement procedure," J. Acoust. Soc. Am. **63**, 559–566.

Quraishi, I. H., and Raphael, R. M. (**2008**). "Generation of the endocochlear potential: A biophysical model," Biophys. J. **94**, L64–66.

Salt, A. N., Brown, D. J., Hartsock, J. J., and Plontke, S. K. (**2009**). "Displacements of the organ of Corti by gel injections into the cochlear apex," Hear. Res. **250**, 63–75.

Salt, A. N., and DeMott, J. E. (**1999**). "Longitudinal endolymph movements and endocochlear potential changes induced by stimulation at infrasonic frequencies," J. Acoust. Soc. Am. **106**, 847–856.

Salt, A. N., and Hullar, T. E. (**2010**). "Responses of the ear to low frequency sounds, infrasound and wind turbines," Hear. Res. **268**, 12–21.

Schmiedt, R. A., Lang, H., Okamura, H. O., and Schulte, B. A. (**2002**). "Effects of furosemide applied chronically to the round window: A model of metabolic presbyacusis," J. Neurosci. **22**, 9643–9650.

Sewell, W. F. (**1984**). "The effects of furosemide on the endocochlear potential and auditory-nerve fiber tuning curves in cats," Hear. Res. **14**, 305–314.

Sirjani, D. B., Salt, A. N., Gill, R. M., and Hale, S. A. (**2004**). "The influence of transducer operating point on distortion generation in the cochlea," J. Acoust. Soc. Am. **115**, 1219–1229.

Van den Berg, G. P. (**2006**). "The sound of high winds: The effect of atmospheric stability on wind turbine sound and microphone noise," Ph.D. dissertation, University of Groningen, Netherlands. http://dissertations.ub.rug.nl/faculties/science/2006/g.p.van.den.berg/ (Last viewed 8/3/2012).

von Békésy, G. (**1951**). "Microphonics produced by touching the cochlear partition with a vibrating electrode," J. Acoust. Soc. Am. **23**, 18–28.

von Békésy, G. (**1960**). *Experiments in Hearing* (McGraw-Hill, New York), pp. 672–682.

Walloch, R. A., and Taylor-Spikes, M. (**1976**). "Auditory thresholds in the guinea pig: A preliminary report of a behavioral technique employing a food reward," Laryngoscope **86**, 1699–1705.

West, C. D. (**1985**). "The relationship of the spiral turns of the cochlea and the length of the basilar membrane to the range of audible frequencies in ground dwelling mammals," J. Acoust. Soc. Am. **77**, 1091–1101.

Whitfield, I. C., and Ross, H. F. (**1965**). "Cochlear microphonic and summating potentials and the outputs of individual hair cell generators," J. Acoust. Soc. Am. **18**, 401–408.

Wilson, J. P., and Johnstone, J. R. (**1975**). "Basilar membrane and middle-ear vibration in guinea pig measured by capacitive probe," J. Acoust. Soc. Am. **57**, 705–723.